The Astrophysical Journal Letters, 815:L8 (6pp), 2015 December 10 doi:10.1088/2041-8205/815/1/L8

ALMA DEEP FIELD IN SSA22: A CONCENTRATION OF DUSTY STARBURSTS IN A $z = 3.09$ PROTOCLUSTER CORE

H. Umehata[1,2], Y. Tamura[2], K. Kohno[2,3], R. J. Ivison[1,4], D. M. Alexander[5], J. E. Geach[6], B. Hatsukade[7], D. H. Hughes[8], S. Ikarashi[9], Y. Kato[7,10], T. Izumi[2], R. Kawabe[7,11,12], M. Kubo[13], M. Lee[7,10], B. Lehmer[14], R. Makiya[2], Y. Matsuda[7,11], K. Nakanishi[7,11], T. Saito[7], I. Smail[5], T. Yamada[15], Y. Yamaguchi[2], and M. Yun[8]

[1] European Southern Observatory, Karl-Schwarzschild-Str. 2, D-85748 Garching, Germany; humehata@eso.org
[2] Institute of Astronomy, School of Science, The University of Tokyo, 2-21-1 Osawa, Mitaka, Tokyo 181-0015, Japan
[3] Research Center for the Early Universe, The University of Tokyo, 7-3-1 Hongo, Bunkyo, Tokyo 113-0033, Japan
[4] Institute for Astronomy, University of Edinburgh, Royal Observatory, Blackford Hill, Edinburgh EH9 3HJ, UK
[5] Centre for Extragalactic Astronomy, Department of Physics, Durham University, South Road, Durham DH1 3LE, UK
[6] Centre for Astrophysics Research, Science & Technology Research Institute, University of Hertfordshire, Hatfield AL10 9AB, UK
[7] National Astronomical Observatory of Japan, 2-21-1 Osawa, Mitaka, Tokyo 181-8588, Japan
[8] Department of astronomy, University of Massachusetts, Amherst, MA 01003, USA
[9] Kapteyn Astronomical Institute, University of Groningen, P.O. Box 800, 9700AV Groningen, The Netherlands
[10] Department of Astronomy, Graduate school of Science, The University of Tokyo, 7-3-1 Hongo, Bunkyo-ku, Tokyo 133-0033, Japan
[11] Department of Astronomy, School of Science, The Graduate University for Advanced Studies (SOKENDAI), Osawa, Mitaka, Tokyo 181-8588, Japan
[12] Joint ALMA Observatory, Alonso de Cordova 3107 Vitacura, Santiago 763 0355, Chile
[13] Institute for Cosmic Ray Research, University of Tokyo, 5-1-5 Kashiwa-no-Ha, Kashiwa City, Chiba 277-8582, Japan
[14] Department of Physics, University of Arkansas, 226 Physics Building, 835 West Dickson Street, Fayetteville, AR 72701, USA
[15] Astronomical Institute, Tohoku University, 6-3 Aoba, Aramaki, Aoba-ku, Sendai, Miyagi 980-8578, Japan
Received 2015 September 21; accepted 2015 October 29; published 2015 December 4

ABSTRACT

We report the results of $1\farcm5 \times 3'$ mapping at 1.1 mm with the Atacama Large Millimeter/submillimeter Array toward the central region of the $z = 3.09$ SSA22 protocluster. By combining our source catalog with archival spectroscopic redshifts, we find that eight submillimeter galaxies (SMGs) with flux densities, $S_{1.1\,\mathrm{mm}} = 0.7$–$6.4$ mJy ($L_{\mathrm{IR}} \sim 10^{12.1}$–$10^{13.1}\,L_{\odot}$) are at $z = 3.08$–3.10. Not only are these SMGs members of the protocluster, but they in fact reside within the node at the junction of the 50 Mpc scale filamentary three-dimensional structure traced by Lyα emitters in this field. The eight SMGs account for a star formation rate density (SFRD) $\sim 10\,M_{\odot}\,\mathrm{yr}^{-1}\,\mathrm{Mpc}^{-3}$ in the node, which is two orders of magnitudes higher than the global SFRD at this redshift. We find that four of the eight SMGs host an X-ray-luminous active galactic nucleus. Our results suggest that the vigorous star formation activity and the growth of supermassive black holes (SMBHs) occurred simultaneously in the densest regions at $z \sim 3$, which may correspond to the most active historical phase of the massive galaxy population found in the core of the clusters in the present universe. Two SMGs are associated with Lyα blobs, implying that the two populations coexist in high-density environments for a few cases.

Key words: galaxies: starburst – large-scale structure of universe – quasars: general

1. INTRODUCTION

In the current framework of cold dark matter (CDM) cosmologies, the formation and evolution of galaxies and supermassive black holes (SMBHs) are closely related to those of cosmic structures on a large scale. The density distribution of dark matter is expected to reflect that of baryonic matter and consequently that of galaxies (e.g., Kauffmann et al. 1999). Therefore, the environment that galaxies inhabit is a crucial key for comprehending galaxy formation and evolution throughout cosmic history. In the local universe, the dense fields, seen as galaxy clusters, are occupied by passive, early-type galaxies, while star-forming, late-type galaxies are seen in less dense fields (e.g., Dressler 1980). Some works argue that the dependence of star formation rate (SFR) on density can be reversed at $z \gtrsim 1$ (e.g., Elbaz et al. 2007). There are contrary claims (e.g., Grützbauch et al. 2011), although these are not based on dust-insensitive tracers of star formation.

Submillimeter galaxies (SMGs; for a recent review, see Casey et al. 2014) are one of the most important populations in unveiling the environmental dependence of galaxy formation on a large scale in the early universe ($z \gtrsim 2$–3). SMGs are massive gas-rich galaxies characterized as being enshrouded by dust and undergoing intense starburst activity (SFR of approximately several 100 to 1000 $M_{\odot}\,\mathrm{yr}^{-1}$; e.g., Swinbank et al. 2014). A fraction of SMGs harbor active galactic nuclei (AGNs), which suggests that SMGs also exist at the growth phase of SMBHs (e.g., Alexander et al. 2005). It has been argued that SMGs are progenitors of massive elliptical galaxies in the local universe (e.g., Eales et al. 1999), and cosmological simulations suggest the growth of the massive ellipticals in high-density regions at $z \gtrsim 2$–3 (e.g., De Lucia et al. 2006). Thus, unveiling the relationship between SMGs and underlying large-scale structures is quite important for understanding the formation history of massive galaxies and large-scale structures.

The SSA22 protocluster at $z = 3.09$, which is considered to be an ancestor of present-day clusters such as Coma (Steidel et al. 1998), is one of the best fields from such a viewpoint. Yamada et al. (2012) conducted a huge narrowband survey to detect $z \sim 3.09$ Lyα emitters (LAEs) in over 2 deg^2 area and found that the density peak in SSA22 is extremely rare and outstanding ($\sim$6 times the average surface density). Other populations such as Lyman break galaxies (LBGs; e.g., Steidel et al. 1998) and distant red galaxies (DRGs; e.g., Uchimoto et al. 2012) are also overabundant in this field. While some submillimeter/millimeter surveys taken with AzTEC/ASTE

(Tamura et al. 2009; Umehata et al. 2014), SCUBA (e.g., Geach et al. 2005; Chapman et al. 2005), and SCUBA2 (Geach et al. 2014) have been conducted in this field, the angular resolution of single-dish telescopes is insufficient in obtaining an accurate picture. We performed wide and deep imaging at 1.1 mm using the Atacama Large Millimeter/submillimeter Array (ALMA) in this field in order to take advantage of its high angular resolution and high sensitivity to conduct an unconfused survey of dusty galaxy activity in this structure and pinpoint the galaxies responsible for it.

In this Letter, we present the first results focusing on the SMGs at $z = 3.09$. The survey design and source catalog of the ALMA observations will be described in more detail in an upcoming paper (H. Umehata et al. 2015, in preparation). Our observations are briefly explained in Section 2. We present the relevant results in Section 3 and discuss the role of the environment in galaxy formation in Section 4. Throughout this Letter, we adopt a cosmology with $\Omega_{\rm m} = 0.3$, $\Omega_\Lambda = 0.7$, and $H_0 = 70\,{\rm km\ s^{-1}\ Mpc^{-1}}$.

2. OBSERVATIONS AND DATA REDUCTION

In ALMA Cycle 2, we observed a $2' \times 3'$ area centered at R.A. (J2000) $= 22^{\rm h}17^{\rm m}34^{\rm s}$, decl. (J2000) $= +00°17'00''$ using 103 discrete pointing fields (Proposal ID 2013.1.00162.S, PI: Umehata). We name this field ALMA Deep Field in SSA22 or ADF22. In this Letter, we report the initial results from 80 pointing data, which roughly correspond to an area of $1.'5 \times 3'$. The observations were carried out during parts of five contiguous nights (2014 June 6–10) using 33–36 12 m antennas. The array configuration was C34–4, which results in baseline lengths of 20–450 m. We utilized the band 6 receiver with the TDM correlator to select a central frequency of 263 GHz (1.1 mm). The on-source time per pointing is 2.0–2.5 minutes. The quasar J2148+0657 was observed for bandpass, amplitude, phase, and flux calibration.

The data were processed with the Common Astronomy Software Application (CASA).[16] The final entire map was created through the "clean" process (with natural weighting and by setting the imager mode to "mosaic" in CASA). The resulting map has a synthesized beam of $0.''53 \times 0.''50$ (P.A. $= -84$ deg) and a typical rms revel of 0.07 mJy beam^{-1}. We utilize a source-finding code, AEGEAN v1.9.5-56 (Hancock et al. 2012), to extract sources on the final mosaic image with a detection threshold of 4σ. The flux densities of the detected sources were measured with CASA task, IMFIT.

3. RESULTS

3.1. Extraction of $z = 3.09$ SMGs

In order to determine redshifts of ALMA sources and extract the members of the $z = 3.09$ structure, we compared our 1.1 mm source catalog with archival catalogs of spectroscopic and photometric redshifts (Chapman et al. 2005; Tamura et al. 2010; Bothwell et al. 2013; Kubo et al. 2015a, 2015b; M. Yun et al. 2015, in preparation). As a result, we yielded eight 1.1 mm sources with $z_{\rm spec} = 3.08$–3.10 and a further SMG with $z_{\rm phot} \sim 3.1$. The positions of these ALMA-selected SMGs are shown in Figure 1.

The archival spectroscopic redshifts are measured from millimeter, near-infrared, and optical spectroscopy. Millimeter spectroscopy of ^{12}CO (3–2) reveals the redshifts for two SMGs. ADF22b is consistent with SMM J221735.15 +001537.2 at $z_{\rm CO} = 3.096$, which was observed with PdBI (Bothwell et al. 2013). In addition, one of the SMGs discovered in the AzTEC/ASTE survey, SSA22-AzTEC1 (hereafter AzTEC1; Umehata et al. 2014), recently has been observed with the Large Millimeter Telescope (LMT) with an effective beam size of $\sim 28''$. Its redshift is $z = 3.092$ if we consider that the detected line is ^{12}CO (3–2) (M. Yun et al. 2015, in preparation). We find that AzTEC1 is split into two sources of ADF22a and ADF22i in our ALMA map. ADF22a has a mid-infrared to radio photo-z of $3.19^{+0.26}_{-0.35}$ (Tamura et al. 2010) and likely dominates the CO emission since it is $3\times$ brighter than ADF22i at 1.1 mm. Thus, we conclude that at least ADF22a is at $z = 3.092$. For ADF22i, we derive an optical to near-infrared photo-z of $3.08^{+0.17}_{-0.15}$ using a method in Umehata et al. (2014).

The spectroscopic redshifts of five SMGs (ADF22d, ADF22e, ADF22f, ADF22g, ADF22h) are determined using near-infrared spectroscopy performed with Subaru/MOIRCS. Kubo et al. (2015a, 2015b) reported the detection of a [O III] λ5007 line for the *Ks*-band counterparts of the five SMGs. We also confirmed that ADF22c coincides with a radio source at $z_{{\rm Ly}\alpha} = 3.089$, which has been considered as the most plausible counterpart of SCUBA06 (SMM J221735.84+001558.9; Chapman et al. 2005). We present the positional relationship between the SMGs and *Ks*-band counterparts in Figure 2. The synthesized beam of our observation and 4σ detection threshold yield an expected astrometric accuracy of $\lesssim 0.''15$ (e.g., Hodge et al. 2013). All SMGs except for ADF22a has *Ks*-band counterparts within $0.''18$ (or $\approx$1.4 kpc at $z \approx 3.09$). Therefore, we concluded that the [O III] and Lyα lines are from the SMGs.

While some of the SMGs harbor an X-ray AGN (Section 3.2), which can substantially contribute to the energetic output at shorter wavelengths (e.g., Gruppioni et al. 2008), $S_{1.1\ {\rm mm}}$ is considered not significantly contaminated by AGNs and hence can be a good tracer of star formation activity. It is known that AGN contribution falls steeply at a rest frame $\gtrsim 40\ \mu$m (e.g., Mullaney et al. 2011), while we observe at a rest frame $\approx 279\ \mu$m. We estimated the potential AGN contribution to $S_{1.1\ {\rm mm}}$ using MIPS 24 μm flux densities ($S_{24\ \mu{\rm m}}$), following D. M. Alexander et al. (2015, in preparation). ADF22e is the brightest at 24 μm ($S_{24\ \mu{\rm m}} = 450 \pm 10\ \mu$Jy; e.g., Webb et al. 2009). Assuming conservatively that $S_{24\ \mu{\rm m}}$ is fully powered by AGN, the predicted $S_{1.1\ {\rm mm}}$ based on the averaged empirical AGN spectral energy distribution (SED) template of Mullaney et al. (2011) is $S_{1.1\ {\rm mm}} \sim 110\ \mu$Jy (or $\sim$11% of the observed flux density). The remaining X-ray SMGs are relatively faint at 24 μm ($\lesssim$100 μJy, e.g.; Webb et al. 2009), which corresponds to $S_{1.1\ {\rm mm}} \lesssim 25\ \mu$Jy. Therefore, the implied AGN contribution to $S_{1.1\ {\rm mm}}$ is $\lesssim$3.5%.

The lack of any other submillimeter/millimeter data with comparable angular resolution prevents one from putting a constraint on dust SEDs. To evaluate the SFR of the SMGs, we calculated the infrared luminosities ($L_{\rm IR}$ [8–1000 μm]) using SED templates of well-studied starburst galaxies, Arp 220 and M82 (GRASIL; Silva et al. 1998), a composite SED of SMGs from the ALESS (Swinbank et al. 2014), and SMM J2135–0201 (the cosmic eyelash; Swinbank et al. 2010) to consider a variety of SEDs. We created best-fit SED for each template based on redshift and $S_{1.1\ {\rm mm}}$. The spectra between 8 and 1000 μm in the rest frame were integrated, and we derive a

[16] http://casa.nrao.edu

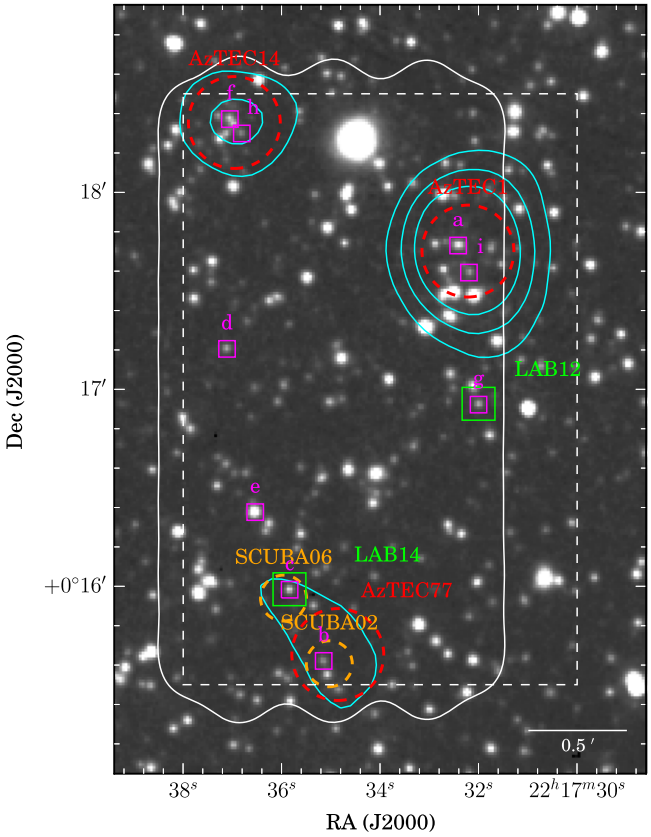

Figure 1. Spatial distributions of SMGs as well as LABs on the IRAC 4.5 μm image. The $5'' \times 5''$ magenta squares represent ALMA sources at $z = 3.09$. The red and orange dashed circles stand for AzTEC/ASTE (Umehata et al. 2014) and SCUBA sources (Scott et al. 2006), which are suggested to be at $z \sim 3.09$ (Chapman et al. 2005; Tamura et al. 2010; Umehata et al. 2014). The diameters of these circles are $28''$ and $14''$, respectively, which correspond to the size of the FWHM of these surveys. The cyan contours show 3.0, 6.0, and 9.0 σ of 1.1 mm emission in the AzTEC map. The dashed white rectangle shows the whole $2' \times 3'$ area of ADF22, and the white contours outline the currently obtained area (the primary beam attenuation is less than 50%). The green boxes show the position of the LABs (Matsuda et al. 2004).

median value as well as minimum/maximum values. We convert $L_{\rm IR}$ to the SFR using ${\rm SFR}/M_\odot\,{\rm yr}^{-1} = 1.0 \times 10^{-10}\,L_{\rm IR}/L_\odot$ (Kennicutt 1998), assuming a Chabrier initial mass function (Chabrier 2003).

3.2. SMGs in the Node of the Cosmic Web

One of the distinguishing characteristics of the SSA22 protocluster at $z = 3.09$ is the existence of a three-dimensional large-scale structure traced by LAEs (Matsuda et al. 2005). Matsuda et al. confirmed that 56 narrowband-selected LAE candidates were actually at $z = 3.06$–3.12 and found that the protocluster seen as two-dimensional density excess of LAEs had a 50 Mpc scale three-dimensional filamentary structure (Figure 3). ADF22 was designed to observe the intersection of the three-dimensional structure, and the spectroscopic redshifts enable one to compare the distribution of SMGs against the large-scale structure three-dimensionally. All eight SMGs with spec-z are distributed in a range of $z = 3.08$–3.10, which is in good agreement with the redshift space of the node of the LAE filamentary structure as illustrated in Figure 3. As noted in Matsuda et al. (2005), the redshifts determined by Lyα emission lines contain uncertainties due to the peculiar velocities and resonant scatterings in the outflowing H I gas. However, the estimated redshift dispersion is predicted to be small ($\sigma_z \sim 0.005$), and therefore the uncertainties are not supposed to matter in the comparison as a whole. ADF22i, which has been selected based on its photo-z, might be also in the node.

To evaluate the overabundance of SMGs in the node quantitatively, we calculate the volume density of the 1.1 mm sources and compare it with the expected value in general fields based on the total IR luminosity. Swinbank et al. (2014) derived the IR luminosity functions of ALMA-selected SMGs using results of the ALESS survey in the ECDF-S. They utilized optical to near-infrared photo-z's (Simpson et al. 2014) and IR luminosities derived from SED fitting to determine that the volume density of SMGs at $z = 2.5$–3.5 is about $4 \times 10^{-6}\,{\rm Mpc}^{-3}$ for $L_{\rm IR} \gtrsim 10^{12.5}\,L_\odot$.[17] Assuming a redshift slice of $z = 3.08$–3.10, the predicted number of SMGs is 1×10^{-3} within this $1'.5 \times 3'$ field, which corresponds to an area of 2.8×5.6 Mpc at $z = 3.09$. There are three SMGs with $z_{\rm spec} = 3.08$–3.10 and $L_{\rm IR} \gtrsim 10^{12.5} L_\odot$ in ADF22 as listed in Table 1, which is three orders of magnitude greater than the number expected for general fields. Thus, the volume density of SMGs is unusually high in the node. We calculate a star formation rate density (SFRD) in the node of $\sim 10\,M_\odot\,{\rm yr}^{-1}\,{\rm Mpc}^{-3}$ considering the eight SMGs with spec-z, which is two orders of magnitude higher than the global SFRD at this redshift (Madau & Dickinson 2014).

[17] We note that some works suggested that ECDF-S could be $\sim\times 2$ underdense compared to other submillimeter surveys (e.g., Swinbank et al. 2014).

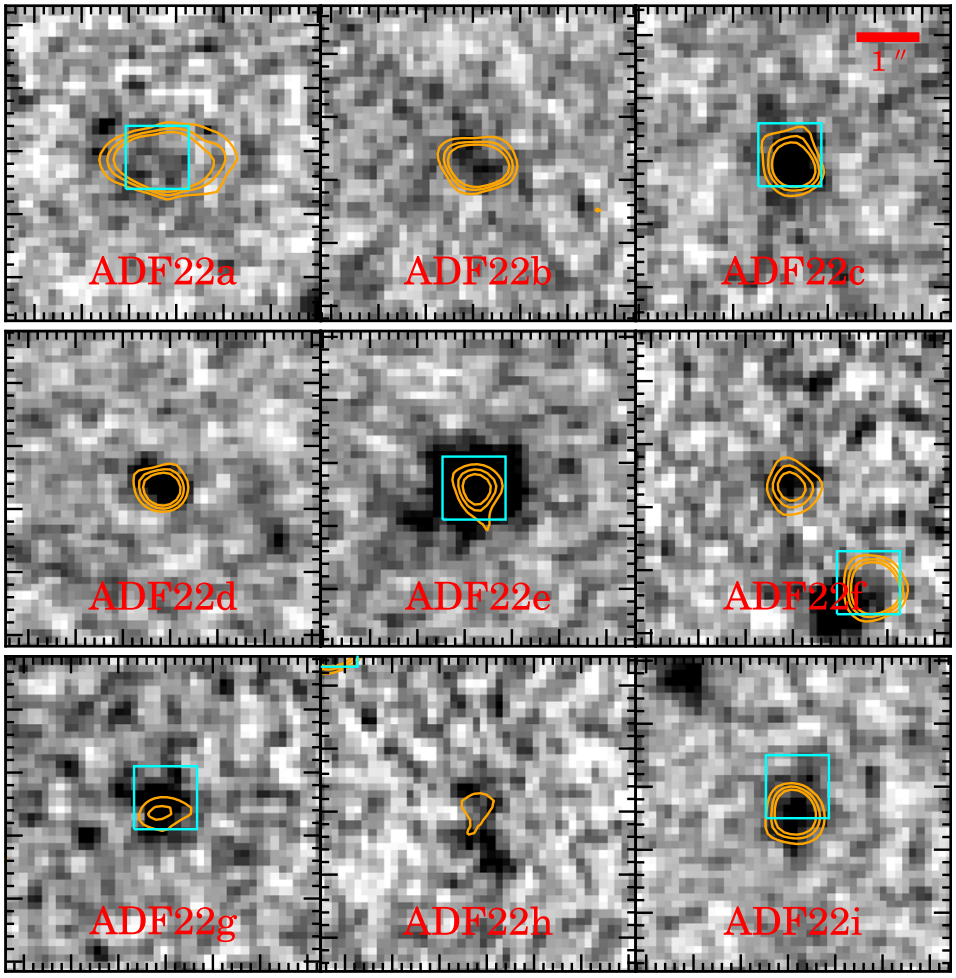

Figure 2. ALMA 1.1 mm contours of $z \simeq 3.09$ SMGs overlaid on the MOIRCS *Ks*-band image. Contours of 3, 6, and 9σ are shown. Cyan squares represent the position of X-ray sources (Lehmer et al. 2009a). Each panel is 5″ square with the ALMA position centered. All the SMGs apart from ADF22a have *Ks*-band counterparts.

In addition to the overabundance, the $z = 3.09$ SMGs in ADF22 are characterized by overlaps with AGNs and Lyα blobs (LABs), which are extended Lyα emitting nebulae. The whole area of ADF22 was observed by *Chandra* at 0.5–2 keV and 2–8 keV (Lehmer et al. 2009a). We found that four SMGs at $z = 3.09$ (ADF22a, ADF22c, ADF22e, ADF22g) have X-ray counterparts listed in Lehmer et al. (2009b) within 0.″5, which means that 50^{+39}_{-24}% of SMGs in the node host X-ray-luminous AGNs with $L_{\rm X} \sim 10^{44}$ erg s^{-1} (Geach et al. 2009; Tamura et al. 2010). ADF22i also has an X-ray counterpart and hence it is one of such AGN-host SMGs. The ALESS survey has comparable depths at submillimeter/millimeter wavelengths compared to ADF22. In the field, Wang et al. (2013) estimated an AGN fraction—a fraction of SMGs containing AGNs—of about 10% for AGNs with rest-frame 0.5–8.0 keV apparent luminosity $\gtrsim 10^{43}$ erg s^{-1}, which is equivalent to that limit at $z = 3.09$ in ADF22 (Lehmer et al. 2009a). Thus, the AGN fraction is relatively high compared with that typically found in the whole SMG population. We also note that there is another X-ray AGN without ALMA detection (J221737.3+001823.2; Kubo et al. 2015). In ADF22, there are 2 of 35 LABs listed in Matsuda et al. (2004). Geach et al. (2009) reported that X-ray counterparts of two SMGs (ADF22c, ADF22g) were associated with the two LABs (LAB14, LAB12), respectively. In other words, two SMGs in the node are found to be associated with LABs.

4. DISCUSSION AND CONCLUSIONS

There is vigorous debate on the environmental dependence on SMG formation at $z \gtrsim 2$, the peak era of cosmic star formation activity. Some studies show that a handful of SMGs at $z = 4$–5 coexist with other star-forming galaxies such as LBGs and argue that SMGs are at protoclusters (e.g., Daddi et al. 2009; Capak et al. 2011). Recent submillimeter/millimeter surveys performed with single-dish telescopes unveil the possible excess of SMGs at $z = 2$–3 toward the known overdense fields (e.g., Tamura et al. 2009; Umehata et al. 2014; Dannerbauer et al. 2014) or a serendipitously found protocluster (Casey et al. 2015). On the other hand, Chapman et al. (2009) and Miller et al. (2015) suggest that SMGs are poor tracers of massive protoclusters and they can reside in less dense environments at least at $z = 2$–2.5.

There have been some obstacles to resolving this issue. First, there is ambiguity in the definition of a protocluster in terms of protocluster mass and the degree of galaxy assembly. Second, the angular resolution of a single-dish telescope is generally insufficient for identifying counterparts in other wavelength images reliably. Third, the *evolution* of the relationship

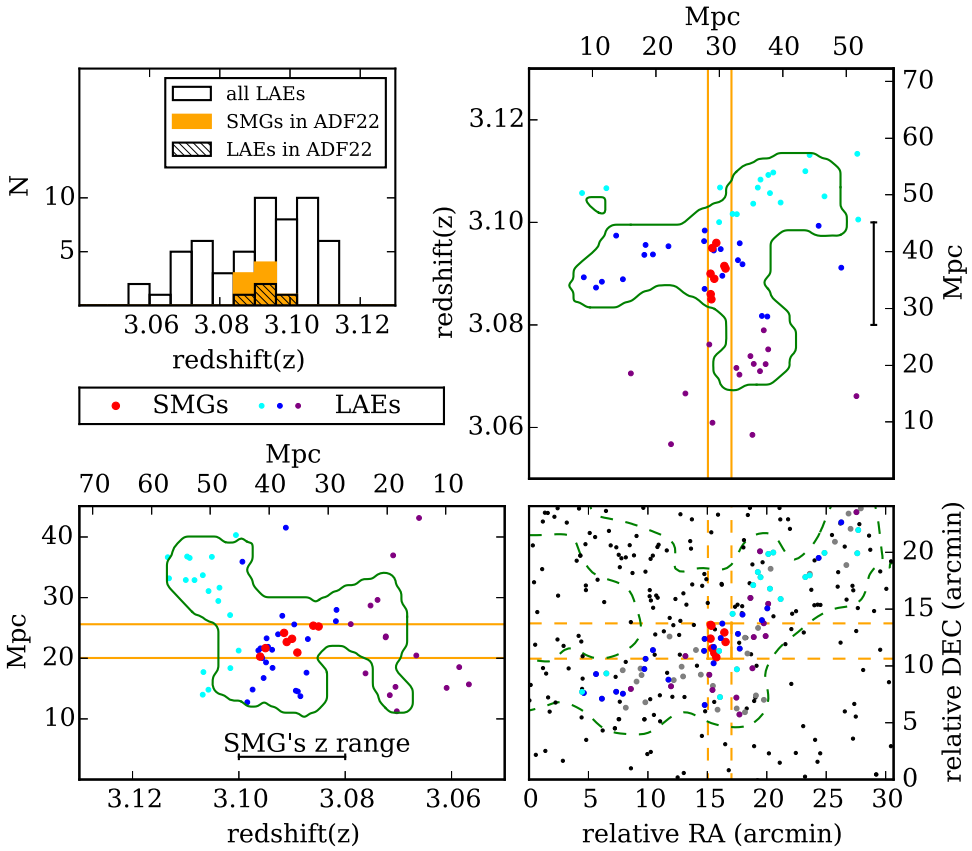

Figure 3. (top left) Redshift distributions of eight SMGs and four LAEs in ADF22 overlaid on that of 56 LAEs in the SSA22 field (Matsuda et al. 2005). (top right, left, and right bottom) Three-dimensional distributions of SMGs in ADF22 (big red circles) and narrowband-selected LAEs in the SSA22 field (small colored circles; Matsuda et al. 2005). The solid (dashed) green lines show the projected contour of the local volume (surface) density of the LAEs. For more details, please see Matsuda et al. (2005). The eight SMGs are concentrated in the intersection of the LAE filamentary structure.

Table 1
$z = 3.09$ SMGs in ADF22

ADF22 ID	Name	z	Type	$S_{\rm peak}$/N	$S_{1.1\ \rm mm}$ (mJy)	log ($L_{\rm IR}$) ($L_\odot$)	SFR$_{\rm IR}$ ($M_\odot$ yr^{-1})	X-ray AGN
ADF22a	ALMAJ221732.41+001743.8	3.092	^{12}CO(3–2) (1)	38.8	6.4 ± 0.2	$13.1^{+0.2}_{-0.1}$	1180^{+890}_{-230}	Y
ADF22b	ALMAJ221735.15+001537.3	3.096	^{12}CO(3–2) (2)	23.8	2.3 ± 0.1	$12.6^{+0.2}_{-0.1}$	420^{+320}_{-80}	N
ADF22c	ALMAJ221735.83+001559.0	3.089	Lyα (3)	16.6	1.8 ± 0.1	$12.5^{+0.2}_{-0.1}$	330^{+250}_{-50}	Y
ADF22d	ALMAJ221737.11+001712.4	3.090	[O III]λ5007 (4)	15.2	1.1 ± 0.1	$12.3^{+0.2}_{-0.1}$	200^{+150}_{-40}	N
ADF22e	ALMAJ221736.54+001622.7	3.095	[O III]λ5007 (4)	11.3	1.0 ± 0.1	$12.3^{+0.2}_{-0.1}$	180^{+140}_{-35}	Y
ADF22f	ALMAJ221737.05+001822.4	3.086	[O III]λ5007 (5)	10.2	1.1 ± 0.1	$12.3^{+0.2}_{-0.1}$	200^{+150}_{-40}	N
ADF22g	ALMAJ221732.01+001655.4	3.091	[O III]λ5007 (4)	5.8	0.7 ± 0.1	$12.1^{+0.2}_{-0.1}$	130^{+100}_{-24}	Y
ADF22h	ALMAJ221736.81+001818.1	3.085	[O III]λ5007 (4)	4.3	0.8 ± 0.2	$12.2^{+0.2}_{-0.1}$	150^{+110}_{-30}	N
ADF22i	ALMAJ221732.19+001735.6	$(3.08^{+0.17}_{-0.15})$	photo-z	17.7	2.0 ± 0.1	$12.6^{+0.2}_{-0.1}$	370^{+280}_{-70}	Y

Note. References of redshifts are: (1) M. Yun et al. (2015, in preparation), (2) Bothwell et al. (2013), (3) Chapman et al. (2005), (4) Kubo et al. (2015a), (5) Kubo et al. (2015b). Photo-z of ADF22i is estimated in a similar way in Umehata et al. (2014). For the column of X-ray AGN, Y means SMGs that host an X-ray-luminous AGN (rest-frame 0.5–8.0 keV apparent luminosity $\gtrsim 10^{43}$ erg s^{-1}; Lehmer et al. 2009a). N represent SMGs without a detectable X-ray counterpart.

between SMGs and environment has not been characterized well, although the protocluster mass scale and star formation in member galaxies are expected to strongly evolve through the era in which SMGs have been observed ($1 \lesssim z \lesssim 6$; e.g., Casey et al. 2014).

The $z = 3.09$ SSA22 protocluster is a preferable target in unveiling whether SMGs are formed in high-density environments at the epoch by virtue of having a remarkable large-scale structure. As described above, our results from ADF22 provide significant observational evidence on the site of SMG formation. Our finding, an overabundance of SMGs in ADF22, is in line with that of the previous works that claim that the associations of SMGs trace the dense environment. Furthermore, it might be suggested that SMGs are preferentially formed around the intersections of the cosmic filamentary structure, though we should note that our ALMA view is limited to only the central part. The existence of a number of SMGs at the $z = 3.09$ protocluster core is also suggestive in considering the evolution of the relationship between SMGs and (proto)clusters. Smail et al. (2014) reported that SMGs are

located at the less dense parts in a $z = 1.6$ cluster, mainly based on their SCUBA2 observations, and the very central area is occupied by the most massive red quiescent galaxies. Meanwhile, Ma et al. (2015) find an excess of SCUBA2 sources in a cluster at $z = 1.5$, suggesting a variety of environments associated with SMG activity at $z < 2$. In contrast to such a result at a relatively low redshift, the SSA22 protocluster at $z = 3.09$ seems to be in a phase in which the most intense starbursts occur at the core. The overabundance of SCUBA sources around high-redshift radio galaxies at $z \sim 3$, which are considered to be signposts of high-density peaks, could show similar phases (e.g., Ivison et al. 2000; Smail et al. 2003), though a shortage of angular resolution and a deficit of redshift information prevent further comparison. These case studies indicate that we might be seeing the exact growth phase of stellar components as well as SMBHs of the massive ellipticals seen in the core of the present-day clusters, and the site where the most active populations reside would evolve from the center to outer parts at decreasing redshifts.

The other important aspect of the nature of SMGs in the node is a correlation between SMGs and other populations. First, the SMGs in ADF22 are frequently associated with AGNs. Our results suggest that the unique environment, the intersection of the large-scale structure, can lead to this trend. Some ideas previously presented; both of accelerated infall of gas and a higher rate of mergers are naturally expected in overdense environments (e.g., De Lucia et al. 2006), which might account for the overabundance of dusty starbursts and their high AGN fraction. Additionally, ALMA imaging helps us uncover obscured star-forming cores embedded in LABs. Intense star formation activities and/or AGNs are supposed to be the possible origins of the extended Lyα emission (e.g., Taniguchi & Shioya 2000) and therefore a connection between SMGs and LABs has been considered. We identify two X-ray-luminous SMGs associated with LABs, which shows that star formation and/or AGNs in SMGs can be related to LABs at least for some cases. On the other hand, the majority of SMGs do not seem to be accompanied by giant Lyα nebulae in their active starburst phase, while both populations inhabit high-density environments.

We thank the anonymous referee gratefully. This Letter makes use of the following ALMA data: ADS/JAO. ALMA#2013.1.00162.S (PI: H. Umehata). ALMA is a partnership of ESO (representing its member states), NSF (USA) and NINS (Japan), together with NRC (Canada) and NSC and ASIAA (Taiwan) and KASI (Republic of Korea), in cooperation with the Republic of Chile. The Joint ALMA Observatory is operated by ESO, AUI/NRAO and NAOJ. H.U., Y.M. were supported by the ALMA Japan Research Grant of NAOJ Chile Observatory, NAOJ-ALMA-0071, 0086. H.U., M.L. are thankful for the JSPS fellowship. Y.M., B.H. acknowledge support from JSPS KAKENHI grant numbers 20647268 and 15K17616. R.J.I. acknowledges support from ERC in the form of the Advanced Investigator Programme, 321302, COSMICISM. I.R.S. acknowledges support from STFC (ST/L00075x/1), the ERC Advanced Investigator program DUSTYGAL 321334, and a Royal Society/Wolfson Merit Award. This work is based in part on archival data obtained with the NASA *Spitzer Space Telescope*.

Facilities: ALMA, Subaru (MOIRCS), CXO (ASIS-I), *Spitzer* (IRAC).

REFERENCES

Alexander, D. M., Bauer, F. E., Chapman, S. C., et al. 2005, ApJ, 632, 736
Bothwell, M. S., Smail, I., Chapman, S. C., et al. 2013, MNRAS, 429, 3047
Capak, P. L., Riechers, D., Scoville, N. Z., et al. 2011, Natur, 470, 233
Casey, C. M., Cooray, A., Capak, P., et al. 2015, ApJL, 808, L33
Casey, C. M., Narayanan, D., & Cooray, A. 2014, PhR, 541, 45
Chabrier, G. 2003, PASP, 115, 763
Chapman, S. C., Blain, A., Ibata, R., et al. 2009, ApJ, 691, 560
Chapman, S. C., Blain, A. W., Smail, I., & Ivison, R. J. 2005, ApJ, 622, 772
Daddi, E., Dannerbauer, H., Stern, D., et al. 2009, ApJ, 694, 1517
Dannerbauer, H., Kurk, J. D., De Breuck, C., et al. 2014, A&A, 570, A55
De Lucia, G., Springel, V., White, S. D. M., Croton, D., & Kauffmann, G. 2006, MNRAS, 366, 499
Dressler, A. 1980, ApJ, 236, 351
Eales, S., Lilly, S., Gear, W., et al. 1999, ApJ, 515, 518
Elbaz, D., Daddi, E., Le Borgne, D., et al. 2007, A&A, 468, 33
Geach, J. E., Alexander, D. M., Lehmer, B. D., et al. 2009, ApJ, 700, 1
Geach, J. E., Bower, R. G., Alexander, D. M., et al. 2014, ApJ, 793, 22
Geach, J. E., Matsuda, Y., Smail, I., et al. 2005, MNRAS, 363, 1398
Gruppioni, C., Pozzi, F., Polletta, M., et al. 2008, ApJ, 684, 136
Grützbauch, R., Conselice, C. J., Bauer, A. E., et al. 2011, MNRAS, 418, 938
Hancock, P. J., Murphy, T., Gaensler, B. M., Hopkins, A., & Curran, J. R. 2012, MNRAS, 422, 1812
Hodge, J. A., Carilli, C. L., Walter, F., Daddi, E., & Riechers, D. 2013, ApJ, 776, 22
Ivison, R. J., Dunlop, J. S., Smail, I., et al. 2000, ApJ, 542, 27
Kauffmann, G., Colberg, J. M., Diaferio, A., & White, S. D. M. 1999, MNRAS, 307, 529
Kennicutt, R. C., Jr. 1998, ARA&A, 36, 189
Kubo, M., Yamada, T., Ichikawa, T., et al. 2015a, ApJ, 799, 38
Kubo, M., Yamada, T., Ichikawa, T., et al. 2015b, MNRAS, in press (arXiv:1510.04816)
Lehmer, B. D., Alexander, D. M., Chapman, S. C., et al. 2009a, MNRAS, 400, 299
Lehmer, B. D., Alexander, D. M., Geach, J. E., et al. 2009b, ApJ, 691, 687
Ma, C.-J., Smail, I., Swinbank, A. M., et al. 2015, ApJ, 806, 257
Madau, P., & Dickinson, M. 2014, ARA&A, 52, 415
Matsuda, Y., Yamada, T., Hayashino, T., et al. 2004, AJ, 128, 569
Matsuda, Y., Yamada, T., Hayashino, T., et al. 2005, ApJL, 634, L125
Miller, T. B., Hayward, C. C., Chapman, S. C., & Behroozi, P. S. 2015, MNRAS, 452, 878
Mullaney, J. R., Alexander, D. M., Goulding, A. D., & Hickox, R. C. 2011, MNRAS, 414, 1082
Scott, S. E., Dunlop, J. S., & Serjeant, S. 2006, MNRAS, 370, 1057
Silva, L., Granato, G. L., Bressan, A., & Danese, L. 1998, ApJ, 509, 103
Simpson, J. M., Swinbank, A. M., Smail, I., et al. 2014, ApJ, 788, 125
Smail, I., Geach, J. E., Swinbank, A. M., et al. 2014, ApJ, 782, 19
Smail, I., Ivison, R. J., Gilbank, D. G., et al. 2003, ApJ, 583, 551
Steidel, C. C., Adelberger, K. L., Dickinson, M., et al. 1998, ApJ, 492, 428
Swinbank, A. M., Simpson, J. M., Smail, I., et al. 2014, MNRAS, 438, 1267
Swinbank, A. M., Smail, I., Longmore, S., et al. 2010, Natur, 464, 733
Tamura, Y., Iono, D., Wilner, D. J., et al. 2010, ApJ, 724, 1270
Tamura, Y., Kohno, K., Nakanishi, K., et al. 2009, Natur, 459, 61
Taniguchi, Y., & Shioya, Y. 2000, ApJL, 532, L13
Uchimoto, Y. K., Yamada, T., Kajisawa, M., et al. 2012, ApJ, 750, 116
Umehata, H., Tamura, Y., Kohno, K., et al. 2014, MNRAS, 440, 3462
Wang, S. X., Brandt, W. N., Luo, B., et al. 2013, ApJ, 778, 179
Webb, T. M. A., Yamada, T., Huang, J.-S., et al. 2009, ApJ, 692, 1561
Yamada, T., Nakamura, Y., Matsuda, Y., et al. 2012, AJ, 143, 79